Detection of Ionospheric Scintillation in GNSS data over the Faroe Islands during a solar-min

Gethin Wyn ROBERTS, Faroe Islands

Key words: GNSS, ionospheric scintillation, solar-min

SUMMARY

During the 7 October 2018, a visible aurora borealis was witnessed over the Faroe Islands (62°N) at 20:00 for a period of around 30 minutes. GNSS data from a CORS GNSS receiver in Tórshavn, gathering data at a rate of 1Hz was investigated on the 6, 7 and 8 October in order to study the effect during this event on GNSS carrier phase and code measurements. Two approaches were used, these being the Time Differenced Code Minus Carrier and the Time Differenced Phase Ionospheric Residual techniques. The first technique predominately identifies noise in the code measurements, whilst the second identifies relative noise in carrier phase observables. The results illustrate that the carrier phase measurements are affected by the event, but not so much the code measurements. Not all the satellites were affected, and individual satellites were affected at disparate time instances as the plasma cloud passed across the ionosphere. The results illustrate that the location of the cloud can be calculated at any time using all 31 GNSS satellites observed during the 30-minute period, which give a relatively dense product. These approaches can be used to eliminate satellites that are affected at specific instances in a positioning solution. Comparisons are made between the GNSS results and 1Hz geomagnetic readings taken at Suðuroy in the Faroe Islands, illustrating correlations.

The GPS data were positioned using both AUSPOS and CSRS-PPP. The results illustrate that the positional error during the aurora borealis event reached over 1m when using AUSPOS and 0.8m using CSRS-PPP.

This occurrence was during a solar-min. In 5 years time, we will reach a solar-max, where ionospheric activities and scintillation will increase in number and magnitude. Such phenomena will greatly affect high latitudes and equatorial regions, and techniques are required to detect how the data of individual GNSS satellites are affected in real time. In addition, other electromagnetic signals will be affected, and knowing the real time location of a plasma cloud causing scintillation will be useful.

Detection of Ionospheric Scintillation in GNSS data over the Faroe Islands during a solar-min.

Gethin Wyn ROBERTS, Faroe Islands

1. INTRODUCTION

Global Navigation Satellite System (GNSS) signals travel through the ionosphere to reach the earth. As they pass through the ionosphere, the signals are interfered with, causing the carrier phase to advance and the code measurements to be delayed in their arrival. These perturbations are frequency dependent, therefore, linear combinations of either the code or carrier phase observables can be calculated using two or three frequencies which will be virtually free of the effect of the ionosphere (Liu et al. 2018; Fritsche et al. 2005). However, a second effect of the ionosphere exists, known as ionospheric scintillation. Small scale irregularities in the density and movement of free electrons in the ionosphere cause rapid and random fluctuations in the GNSS signals after propagating through these plasma inconsistencies. These perturbations can result in the signal strength reducing, leading to the GNSS receiver not being able to acquire and track the signal, and also causing cycle slips (Zhao et al. 2019) in the data due to the phase lock loop of the receiver being impinged (Luo et al. 2017).

I investigate the use of ordinary multi-frequency geodetic GNSS receivers in order to identify the effect of scintillation on GNSS data from GPS, BeiDou, Galileo and GLONASS satellites. The dataset covers a three-day period, including a 30-minute duration where an aurora borealis event was visually observed over the Faroe Islands. Two approaches are used to highlight the satellites being affected by the scintillation, and, I investigate the temporal nature of the phenomena. Local noise sources such as multipath are differenced through comparing the noise between adjacent 1 s epochs of data, where the local multipath will negligibly change. Further to this, the GNSS receiver is in a low multipath environment as well as using a geodetic GNSS antenna.

2. METHODOLOGY

I present two methods in order to detect ionospheric irregularities. The first method, known as the Time Differenced Code-Minus-Carrier (TCMC), calculates the difference in range calculated using the code measurements (measured in metres) and the carrier phase (measured in cycles) values for an individual satellite on the same frequencies (Roberts et al. 2019; de Bakker et al. 2009; Huang et al. 2016; Jiang et al. 2017; Roberts 1997). The change in the difference is compared over successive epochs of data. The carrier phase is scaled into units of metres through multiplying by the wavelength of the respective carrier (λ).

$$TCMC_{(i)}^{(f)} = \left(PR^{(f)} - \lambda\emptyset^{(f)}\right)_{(i)} - \left(PR^{(f)} - \lambda\emptyset^{(f)}\right)_{(i-1)} \quad (1)$$

where $PR_r^{s\,(f)}$ is the code measured by the GNSS receiver from satellite *s* to receiver *r* on frequency *f* (metres), and $\emptyset_r^{s\,(f)}$ is the carrier phase observable measured by the receiver from satellite *s* to receiver *r* on frequency *f* (cycles). *i* represents the epoch under examination.

The second technique, known as the Time Difference Phase Ionospheric Residual (TPIR) method, scales one carrier phase value ϕ_{f_a} for a specific satellite into the units of a second carrier phase observable ϕ_{f_b} for the same satellite and compares the change in the difference between the two values over successive epochs of data(*i* and *i-1)* (Roberts et al. 2019; Cai et al. 2013; Tang et al. 2017). The difference is due to ionosphere activity when there are no cycle slips present. The slow varying biases in both techniques are removed by differencing adjacent 1 s epochs of data.

$$TPIR_{(i)}^{(f_a)} = \left(\phi_{f_a} - \phi_{f_b} \cdot \left(\frac{f_a}{f_b}\right)\right)_{(i)} - \left(\phi_{f_a} - \phi_{f_b} \cdot \left(\frac{f_a}{f_b}\right)\right)_{(i-1)} \quad (2)$$

An aurora borealis event was observed on the night of the October 7, 2018 at around 20:00 to 20:30 over the Faroe Islands (62.0°N, 6.8°W). At the time, there was one GNSS Continuously Operating Reference Station (CORS) station on the Faroe Islands, gathering data at a rate of 1 Hz. The GNSS receiver is a Trimble NETR9, with a Zephyr 2 (TRM57971.00 TZGD) antenna, housed in a radome. The GNSS receiver provides local RTK reference station data to registered users, and the raw data is processed, analyzed and archived by the Danish Agency for Data Supply and Efficiency. The GNSS receiver has been part of the European Reference Frame network since February 27, 2011 (Bruyninx et al. 2012). The NETR9 GNSS receiver can gather triple frequency data from all four GNSS (GPS, GLONASS, Galileo, BeiDou) as well as the Japanese Quasi-Zenith Satellite System (QZSS).

The ionosphere is mainly affected by the activities of the sun and the geomagnetic field of the earth. This is dominated by the 11-year sunspot cycle. Fig. 1 illustrates the sunspot cycle since 2008, illustrating that this was at a minimum during October 7, 2018. Therefore, the GNSS data should have minimal effect from the ionosphere. However, there are still sporadic events that do cause ionospheric disturbances, but not as many or as powerful as during the peak of the sunspot cycle.

Three consecutive days of data are analysed in order to investigate the effect of the ionospheric disturbances during the aurora borealis phenomena on the GNSS data. These are October 6- 8, 2018, with October 7 including the visible aurora borealis event between approximately 20:00 and 20:30. The data from the NETR9 GNSS receiver were gathered at a 1 Hz sampling rate, and the periods from 19:00 to 22:00 for each of the three days are focused upon. The TCMC and TPIR approaches are used on these periods in order to illustrate the expected noise during a typical situation as well as during the event. MATLAB™ was used to implement the algorithms on the GNSS data, in RINEX 3.02 (Receiver Independent Exchange) format. The raw Trimble T02 data was converted into RINEX 3.02 using the Trimble "Convert to RINEX" software.

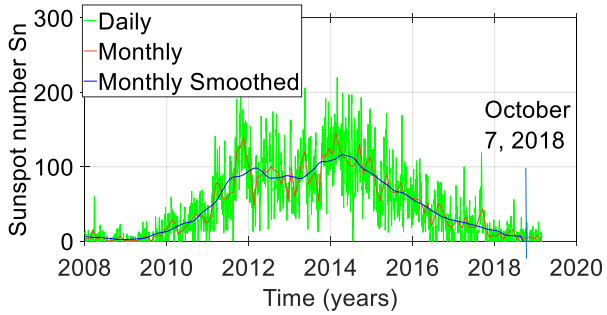

Fig. 1 Sunspot numbers since 2006, illustrating a low period around October 7, 2018. (Source: WDC-SILSO, Royal Observatory of Belgium, Brussels).

3. RESULTS AND DISCUSSION

3.1 TCMC Results

Fig. 2 and 4 illustrate the TCMC values for GPS and Galileo respectively. The satellites considered are only those that are visible during the aurora borealis event (October 7, 2018, 20:00 to 20:30). Other satellites are present in the data files for the period from 19:00 to 22:00 on October 6-8, but not examined. The plots for the TCMC calculated during the time that the aurora borealis was observed, October 7, 2018, are seen in the centre, and the plots for the same period on October 6 and 8 are plotted on the left and right of these, respectively. The satellite numbers are shown on the right of the figures, also including the satellite block type for GPS, Fig. 2. The figures are all plotted at the same scale, thus illustrating the relative noise of all the satellite systems and constellation types. The individual time series have been offset from zero by adding constant values to each of the satellite time series so that the results are distinguished from each other in the figures. The noise comparison, when using both the TCMC and TPIR techniques, of the various GNSS, frequencies, satellite generations, orbit types has already been reported in detail (Roberts 2019). The nominal noise of the TCMC approach can be seen in Fig. 2 and 3 on October 6 and October 8, as well as the results on October 7 away from the period between 20:00 to 20:30, when the aurora borealis phenomena was observed. The data have been closely analysed, including observing whether there are any gaps in the data around the occurrence of the aurora borealis phenomena. On the whole, there were no gaps detected, indicating that the GNSS receiver was able to continuously track the satellites during the presence of scintillation noise. By looking at Fig. 2 and 3 at around 20:00 to 20:30 on October 7, it can be seen that there are anomalies for some of the TCMC results, which are not evident on October 6 and 8.

Fig. 2 illustrates the GPS TCMC time series. It can be seen that the TCMC for GPS L1 (C/A-code) are noisier than the other GPS TCMC values, with the L5 TCMC being the least noisy. PRN30, shows some slight flicker at 20:15 and PRN08 at 20:30 on October 7 on the L5 TCMC plot. However, this is all that is clearly noticeable on the GPS TCMC results. Some of the results include those during the time that specific satellites were seen just above the horizon as they were ascending or descending. Here, the TCMC is expected to become noisier due to the

low elevation angle (Seeber 2003; Circiu et al. 2017), and hence the rapid change in the atmosphere that the signals travel through from epoch to epoch. PRN30, in particular, illustrates this effect, on all three days, as the satellite drops down towards the horizon; the L1C, L2C and L5X TCMC have an increase in noise just after 21:30, but not the L2W signal.

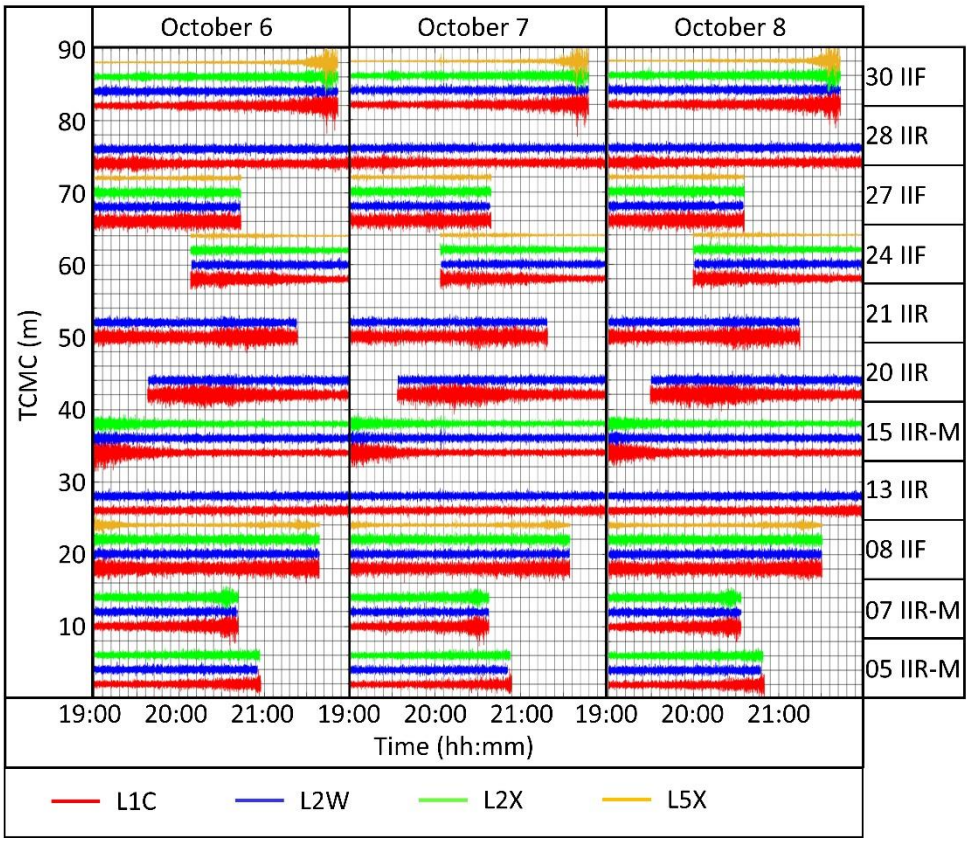

Fig. 2 GPS TCMC, 19:00 to 22:00 on October 6-8, 2018.

Fig. 3 illustrates the TCMC time series for Galileo. It can be seen that the noise of the time series is generally less than GPS (and GLONASS), resulting in more instances where anomalies are seen during the occurrence of the aurora borealis. It can also be seen that the noise of the E5 TCMC is less than the other frequencies. Scintillation noise is more discernible on the E5a, E5b, E5 frequencies, than the E1 frequency. This is due to the E1 code measurement being noisier than the E5a, E5b and E5 code measurements. Anomalies are seen on PRN11, PRN12, PRN19, PRN30, with a slight scintillation on PRN02 on the E5 frequency. Due to the orbital characteristics and orbital revolution period of the Galileo satellites, there is not a good repetition of the same satellites in view on successive days. This is why not all the satellites observed on October 7 are visible on October 6 and 8, during the same time period.

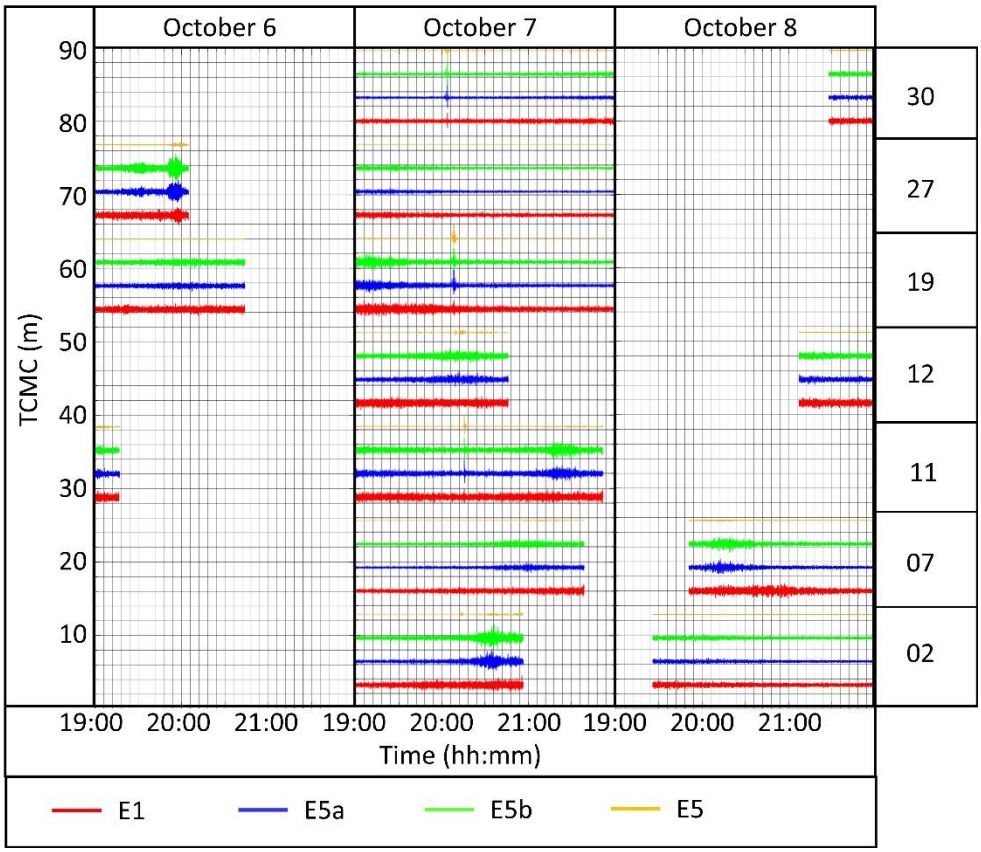

Fig. 3 Galileo TCMC, 19:00 to 22:00 on October 6-8, 2018.

The TCMC results show very little or no scintillation noise. Only for the least noisy TCMC results are some scintillation evident. This all implies that the scintillation mainly affects the carrier phase data and not so much the code measurements, and the noise is only detectable when the TCMC noise, mainly derived from the code measurement noise, is small. Similar results are seen for GLONASS and BeiDou.

3.2 TPIR Results

Fig. 4 and 5 illustrate the TPIR time domain plots for the various frequency combinations for GPS and Galileo respectively, for the October 6 (left) October 7 (centre) and October 8 (right). The satellites considered are only those that are visible during the aurora borealis event (October 7, 2018, 20:00 to 20:30). Other satellites are present in the data files for the period 19:00 to 22:00 during October 6-8, but not presented here, as they don't show any scintillation anomalies on the 7th. Again, the plots have been offset from zero by adding constant values to the results in order to distinguish them from each other in the plots.

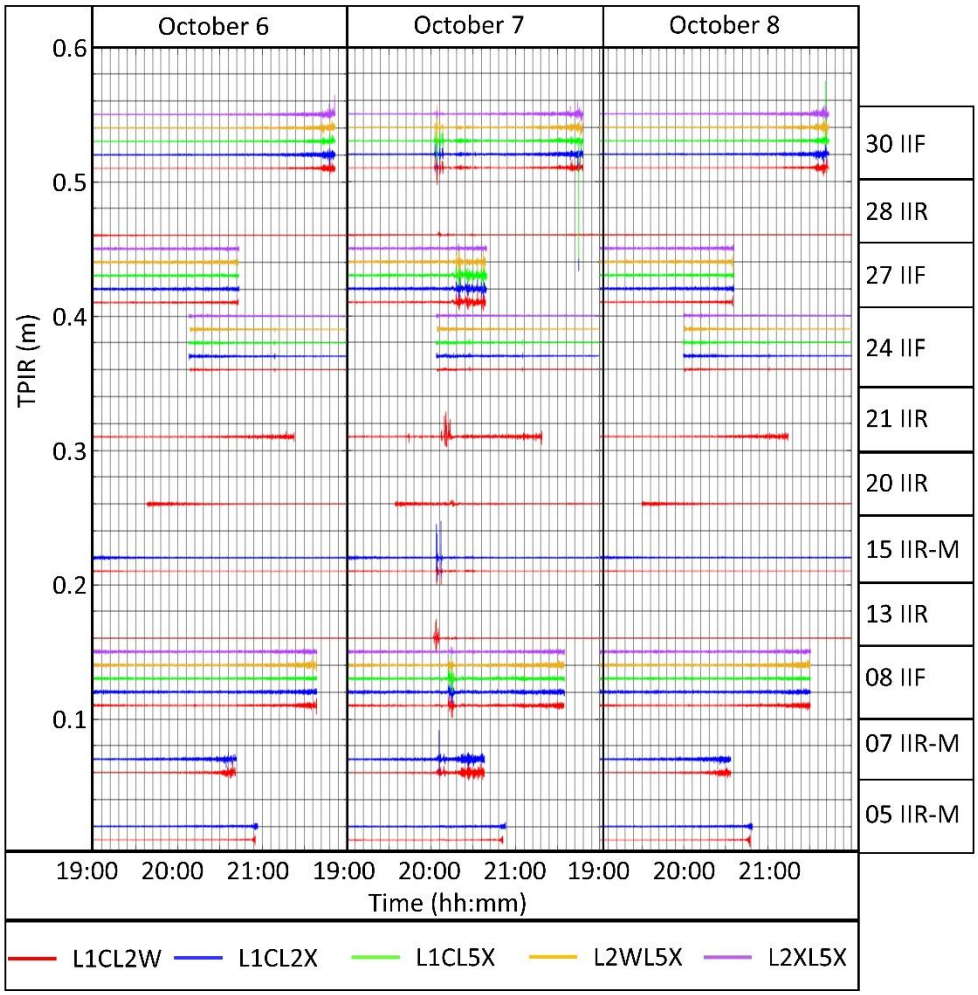

Fig. 4 GPS TPIR, 19:00 to 22:00 on October 6-8, 2018.

Fig. 4 illustrates the GPS TPIR for all 5 of the possible pair combinations. It can be seen that not all the satellites have all the pairs. The block IIR satellites only consist of L1 C/A-code and L2 P(Y)-code related data. Therefore, only one TPIR solution exists (L1C-L2W). The block IIR-M satellites transmit L2 C-code data as well as the L1 C/A-code and L2 P(Y)-code. Therefore, there are two TPIR pair solutions (L1C-L2W and L1C-L2X). The block IIF satellites transmit L5-code related data, as well as L1 C/A-code, L2 P(Y)-code and L2 C-code related data. These correspond to 5 TPIR solutions (L1C-L2W, L1C-L2X, L1C-L5X, L2W-L5X, L2C-L5X). Fig. 4 (left) and Fig. 4 (right) illustrate typical plots when there are no aurora borealis phenomena experienced. Similar to the TCMC results, the plots become noisier if the satellite is rising or setting, such as GPS PRN30 at around 21:40. This time noise is seen on PRN07, PRN08, PRN13, PRN15, PRN20, PRN21, PRN27, PRN28, and PRN30. The magnitude of the scintillation noise varies in from satellite to satellite, as does the time of the occurrences. PRN05 and PRN24 are the only two satellites that display little or no scintillation. At 19:38 there is a slight increase in noise for PRN21.

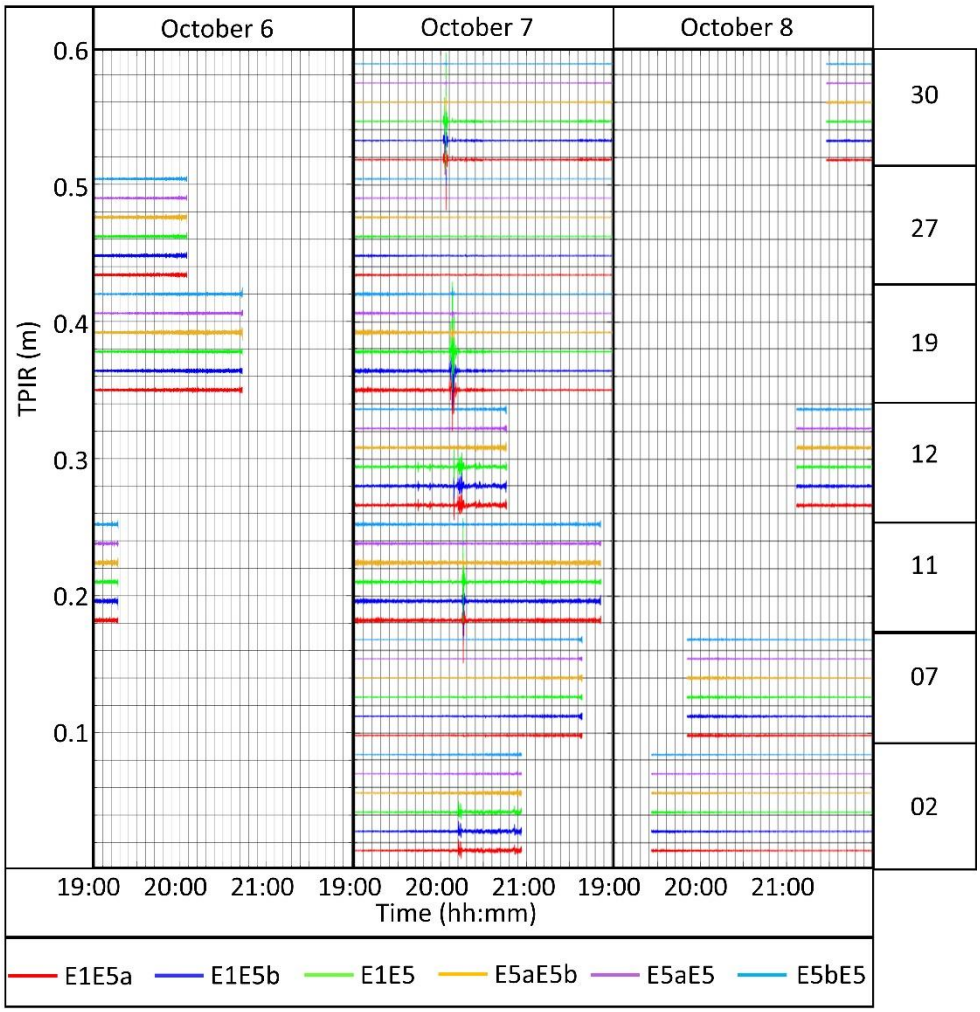

Fig. 5 Galileo TPIR, 19:00 to 22:00 on October 6-8, 2018.

Fig. 5 illustrates the Galileo TPIR time series, illustrating similar results and trends to the other GNSS results. Here, there are 6 possible TPIR combinations (E1-E5a, E1-E5b, E1-E5, E5a-E5b, E5a-E5, E5b-E5). The E1 related TPIR time series are generally noisier and also the scintillation noise is generally larger in magnitude. The occurrences of the scintillation again vary in both terms of magnitude and time between satellites on PRN02, PRN11, PRN12, PRN19 and PRN30. PRN07 and PRN27 do not exhibit scintillation characteristics in the results. At 19:45, a small increase in noise is seen for PRN12 on the E1 related combinations.

The data from the TPIR results are used to calculate the times that the individual satellites are affected by the ionospheric disturbance during October 7, 20:00 to 20:30. The times of the scintillation occurrences are plotted in Fig. 6, every 3 minutes. A ‘cloud’ is drawn around the satellites that are affected at the specific times in order to show the extent of the fallout. It can be seen that the scintillation occurs mainly to the north and also the vicinity of the effect varies rapidly.

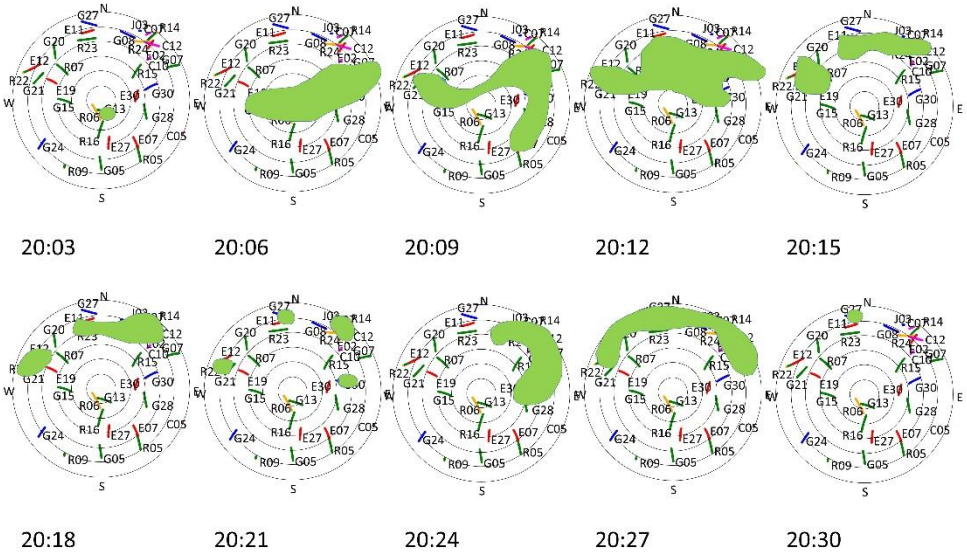

Fig. 6 Extent of the ionospheric disturbance on the GNSS data over a 30 minute period at 3-minute intervals.

The effect of the event is further investigated in two ways. First, geomagnetic values are obtained in order to see if there are anomalies experienced during the same time period, and second, the coordinates of the GNSS station are calculated in order to calculate the coordinate errors.

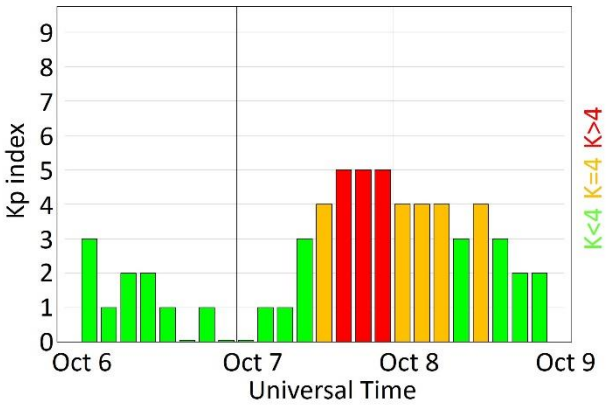

Fig. 7 Kp index values for October 6-8, 2018. (Source: Space Weather Prediction Center, National Oceanic and Atmospheric Administration).

The Kp index has been obtained from the Space Weather Prediction Center of the National Oceanic and Atmospheric Administration, Fig. 7, and the 1Hz geomagnetism data from the Suðuroy station on the Faroe Islands, operated by the Danish Technical University, Fig. 8. The

Kp index (planetary k index) has a 3-hour range and is the mean of 13 geomagnetic observations between 44° and 60° northern and southern geomagnetic latitude. It is an indicator of the disturbance in the magnetic field of the earth. Here it can be seen that the global Kp value does increase to >4 on the evening of October 7. A Kp >4 is required in order to see the northern lights at latitudes such as the Faroe Islands. Further to this, the 1Hz geomagnetism data, located some 20km away, Fig. 8, also show fluctuations around the time of interest. The anomalies in Fig. 8 appear to occur from 15:00 onwards, with the largest jump at 20:00.

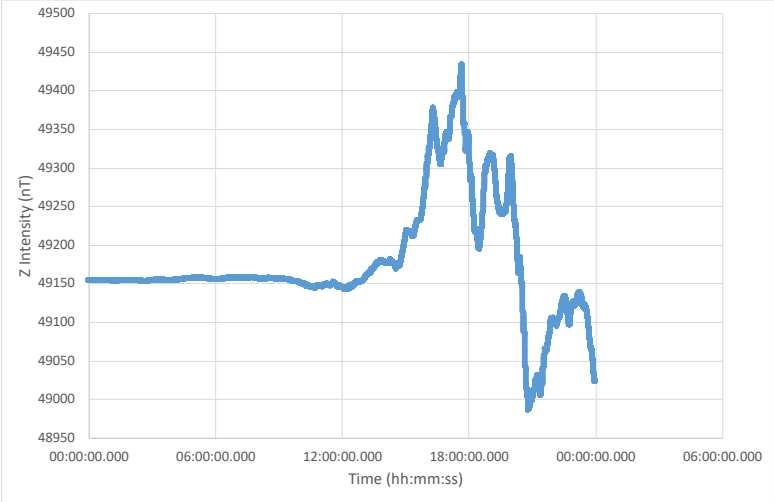

Fig. 8 Geomagnetism data from Suðuroy (Source DTU Space).

Further to this, the GNSS data was used to calculate the coordinates of the station over the three days. At the time, there was currently only one CORS on the whole of the Faroe Islands, and the nearest GNSS CORS receiver is located 366km away in Lerwick, Scotland, which is part of the Ordnance Survey of Great Britain CORS network. Two approaches are used to calculate the coordinates of the GNSS station on the Faroe Islands. First, the 3 days of 1 Hz data were broken down into 1-hour blocks, and a coordinate for every 1 hour was calculated using the Geoscience Australia online GPS processing service (AUSPOS). AUSPOS uses precise ephemerides and International GNSS Service (IGS) stations in order to calculate the coordinates. It is advised that at least 1 hour of data is used when using the facility. AUSPOS uses only GPS data to calculate the coordinates. However, as the GPS constellation repeats itself every sidereal day, this allows a daily comparison, as very little will have changed in terms of geometry and multipath related errors. Fig. 9 (top) illustrates the results, highlighting that there is noise around the time of the scintillation event.

Second, the Natural Resources Canada (NRCan) Canadian Spatial Reference System Precise Point Positioning (CSRS-PPP) online processing service, was used in a kinematic mode to calculate a PPP coordinate every 1 second. CSRS-PPP calculates a PPP solution using IGS precise ephemerides and atmospheric models. It allows a maximum of 24-hours of data to be processed, and only uses GNSS data that has precise ephemerides available at the IGS or NRCan. Again, at the time of the event, Fig. 9 (bottom), there is an increase in the positional

error, highlighted in red. In this solution, however, there are other times when the positional error increases. These include regular spikes at midnight on October 6-8, due to the PPP processing at three individual 24-hour segments. However, the results do show an increase in the positional error at the time of the event. The solution output file for the CSRS-PPP processing indicates that only GPS was used for the solution.

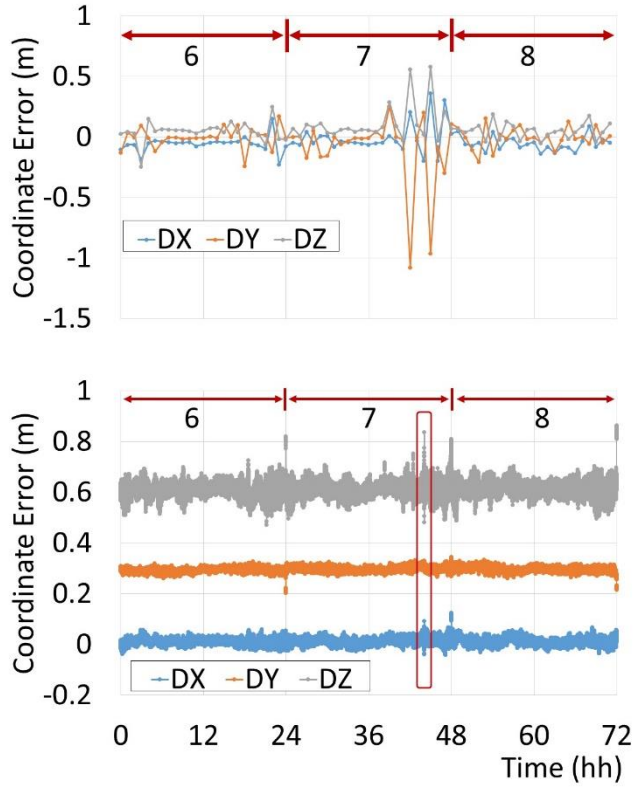

Fig. 9 Effect on 1-hour GNSS Positions calculated using AUSPOS (top), PPP kinematic solution using CSRS-PPP (bottom).

The hourly mean geomagnetism data at Suðuroy, the international Kp values and the resulting coordinates of the GNSS data from the Faroe Islands corroborate that there are anomalies in the geomagnetic, ionospheric and GNSS data. This all helps to illustrate that the TCMC and in particular the TPIR techniques are able to also detect such anomalies. The TPIR can also illustrate where in the sky these temporal scintillation events occur.

Conclusions

Two approaches have been developed and applied in order to investigate the effect that the ionosphere has on GNSS data during a short-lived aurora borealis event. Location-specific multipath noise is cancelled through comparing data between adjacent 1 s epochs. Scintillation is evident in the data, mainly using the TPIR approach, but also when using the TCMC approach when the TCMC noise is low. This implies that only the carrier phase is being affected and not the code measurements.

The scintillation effect can be seen to be both location and time dependent. The extent of the scintillation effect moves across the sky in a matter of minutes. The total time of the event is around 30 minutes and affects the satellites mainly to the north and northeast of the azimuth.

The resulting GNSS data was used to calculate a position solution, which can be seen to consist of coordinate errors around the time of the event. The fiducial positioning solution (AUSPOS) has more error in the results than the PPP solution (CSRS-PPP). GNSS signals are affected by the ionosphere, which is caused by the activities of the sun. The sun permeates through low and high sunspot cycles every 11 years. During October 6-8, 2018 there existed a low period. Such analysis of the noise is paramount, as it can affect the position solution. In 4 or 5 years' time, when the sunspot cycle is at a high, it is expected that there will be more activity such as this. Such ionospheric activity can also affect other electromagnetic frequencies and applications.

Simple analysis, such as those presented, can be used to identify instances when individual satellites are affected by ionospheric scintillation, and hence not use those data in a position solution. This approach can be used in real time, as it only requires the data from the current and previous epoch using normal geodetic GNSS receivers. However, rapid data is required, typically 1 Hz or quicker, as the terms in the observables will become de-correlated over longer intervals, itself causing an increase in noise.

REFERENCES

Bruyninx C, Habrich H, Söhne W, Kenyeres A, Stangl G, Völksen C (2012) Enhancement of the EUREF Permanent Network services and products. Geodesy Planet Earth IAG Symp. 136:27–35. https://doi.org/10.1007/978-3-642-20338-1_4.

Cai, C., Liu, Z., Xia, P., Dai, W. (2013) Cycle slip detection and repair for undifferenced GPS observations under high ionospheric activity. GPS Solut 17(2):247-260. https://doi.org/10.1007/s10291-012-0275-7.

Circiu, M.S., Meurer, M., Felux, M., Gerbeth, D., Thölert, S., Vergara, M., Enneking, C., Sgammini, M., Pullen, S. and Antreich, F. (2017) Evaluation of GPS L5 and Galileo E1 and E5a Performance for Future Multifrequency and Multiconstellation GBAS. Navigation. 64(1):149-163. https://doi.org/10.1002/navi.181.

de Bakker PF, van der Marel H, Tiberius CCJM (2009) Geometry-free undifferenced, single and double differenced analysis of single frequency GPS, EGNOS and GIOVE-A/B measurements. GPS Solut 13(4):305–314. https://doi.org/10.1007/s10291-009-0123-6

Fritsche, M., Dietrich, R., Knöfel, C., Rülke, A., Vey, S., Rothacher, M., and Steigenberger, P. (2005) Impact of higher-order ionospheric terms on GPS estimates. Geophys. Res. Lett. 32(23): L23311. https://doi.org/10.1029/2005GL024342.

Huang, L., Lu, Z., Zhai, G., Ouyang, Y., Huang, M., Lu, X., Wu, T., Li, K. (2016) A new triple-frequency cycle slip detecting algorithm validated with BDS data. GPS Solut. 20(4):761-769. https://doi.org/10.1007/s10291-015-0487-8.

Jiang, Y., Milner, C., Macabiau, C. (2017) Code carrier divergence monitoring for dual-frequency GBAS. GPS Solut 21(2):769-781. https://doi.org/10.1007/s10291-016-0567-4.

Liu, Z., Li, Y., Li, F., Guo, J. (2018) Near real-time PPP-based monitoring of the ionosphere using dual-frequency GPS/BDS/Galileo data. Adv. Space Res. 61(6):1435-1443. doi: https://doi.org/10.1016/j.asr.2017.12.038.

Luo, X., Liu, Z., Lou, Y., Gu, S., Chen, B. (2017) A study of multi-GNSS ionospheric scintillation and cycle-slip over Hong Kong region for moderate solar flux conditions. Adv. Space Res. 6(5):1039-1053. https://doi.org/10.1016/j.asr.2017.05.038.

Roberts, G. W., (1997) Real Time On The Fly Kinematic GPS. Ph.D. Thesis, the University of Nottingham. http://eprints.nottingham.ac.uk/id/eprint/13395

Roberts, G. W. (2019) Noise Comparison of Triple Frequency GNSS Carrier Phase, Doppler and Pseudorange Observables. Measurement 144(2019), 328-344. https://doi.org/10.1016/j.measurement.2019.05.011.

Roberts, G. W., Fossá, S., Jepsen, C. (2019) Temporal characteristics of triple-frequency GNSS scintillation during a visible aurora borealis event over the Faroe Islands amid a period of very low solar activity. GPS Solut 23(89), https://doi.org/10.1007/s10291-019-0881-8

Seeber, G. (2003) Satellite Geodesy: Foundations, Methods, and Applications. 3rd Ed. Walter De Gruyter, Berlin. 240–243.

Tang, L., Zheng, K., Li, X. (2017) Analysis of geometry-free residuals in case of traveling ionosphere disturbances and their impact cycle slip detection. GPS Solut. 21(3):1221-1226. https://doi.org/10.1007/s10291-017-0606-9

Zhao, D., Hancock, C. M., Roberts, G. W., Jin, S. (2019) Cycle Slip Detection during High Ionospheric Activities Based on Combined Triple-Frequency GNSS Signals. Remote Sens. 11(3):250. https://doi.org/10.3390/rs11030250.

ACKNOWLEDGEMENTS

I would like to acknowledge both the Faroese Environment Agency (Umhvørvisstovan) and the Danish Agency for Data Supply and Efficiency (SDFE) for access to the GNSS data. Geoscience Australia and NRCan are also acknowledged for the use of AUSPOS and CSRS-PPP online GNSS processing software. NOAA is acknowledged for access to the Kp values,

and DTU Space (Danish Technical University) is acknowledged for access to the geomagnetism data at Suðuroy.

BIOGRAPHICAL NOTES

Dr Gethin Wyn Roberts is an associate professor at Fróðskaparsetur (University of the Faroe Islands). His research interests are engineering surveying, positioning using GNSS and signal analysis and deformation monitoring. He has published over 270 papers and book chapters in peer reviewed journals and international conferences. He is a past chairman of the FIG's commission 6 "Engineering Surveys", and a Fellow of the Chartered Institution of Civil Engineering Surveyors.

CONTACTS

Dr Gethin Wyn Roberts
University of the Faroe Islands
Tórshavn
FAROE ISLANDS
Email: gethinr@setur.fo
Web site: www.setur.fo